

SUPPLEMENTARY INFORMATION

DEAD-box RNA helicase 10 is required for 18S rRNA maturation by controlling the release of U3 snoRNA from pre-rRNA in embryonic stem cells

Xiuqin Wang, Gongcheng Hu, Lisha Wang, Yuli Lu, Yanjiang Liu, Shengxiong Yang, Junzhi Liao, Qian Zhao, Qiuling Huang, Wentao Wang, Wenjing Guo, Heying Li, Yu Fu, Xiaofei Zhang, Xiangting Wang, Yue-Qin Chen, Xiaorong Zhang, Hongjie Yao*

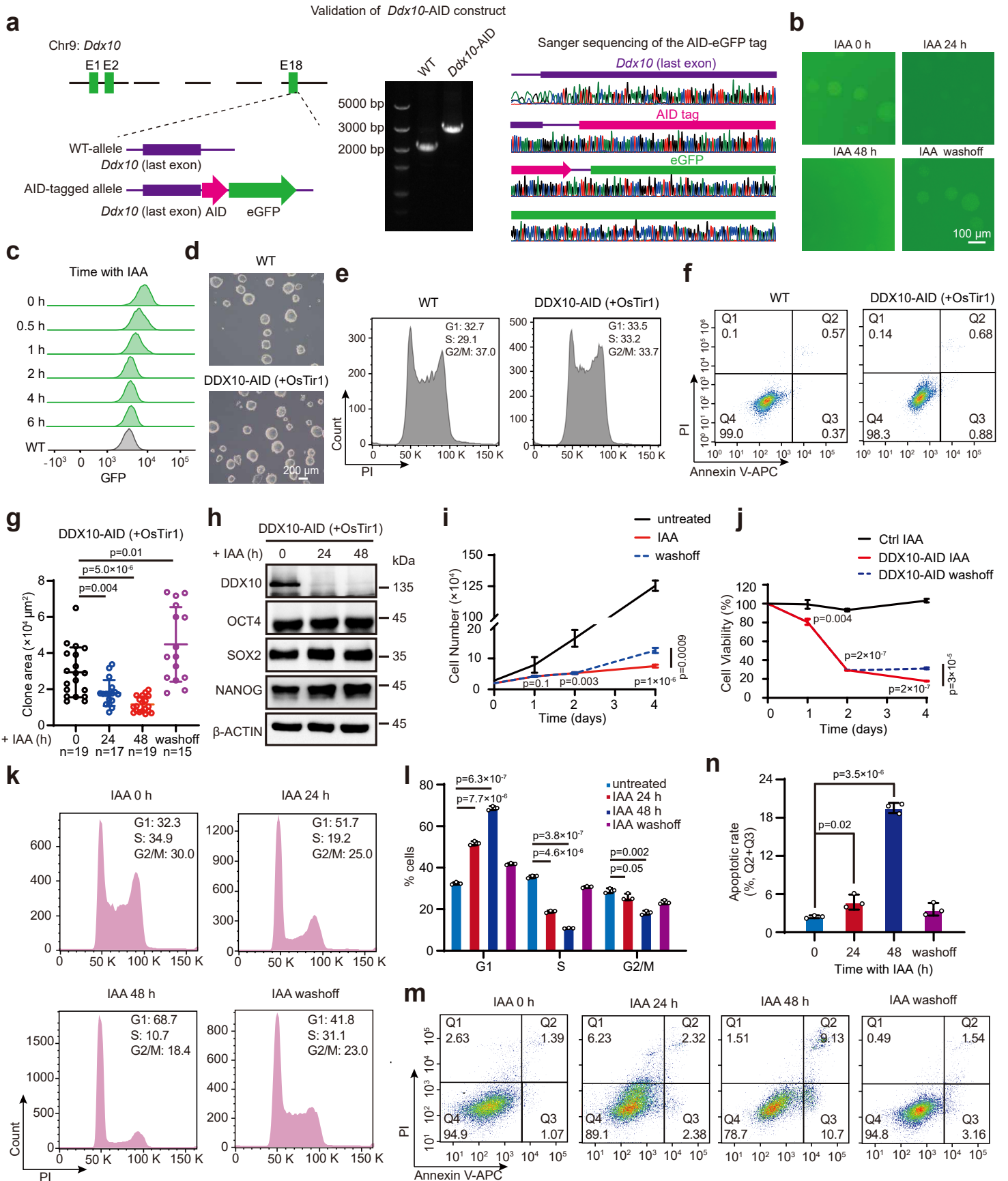
* Corresponding author.

Supplementary information includes:

Supplementary Figures 1-4.

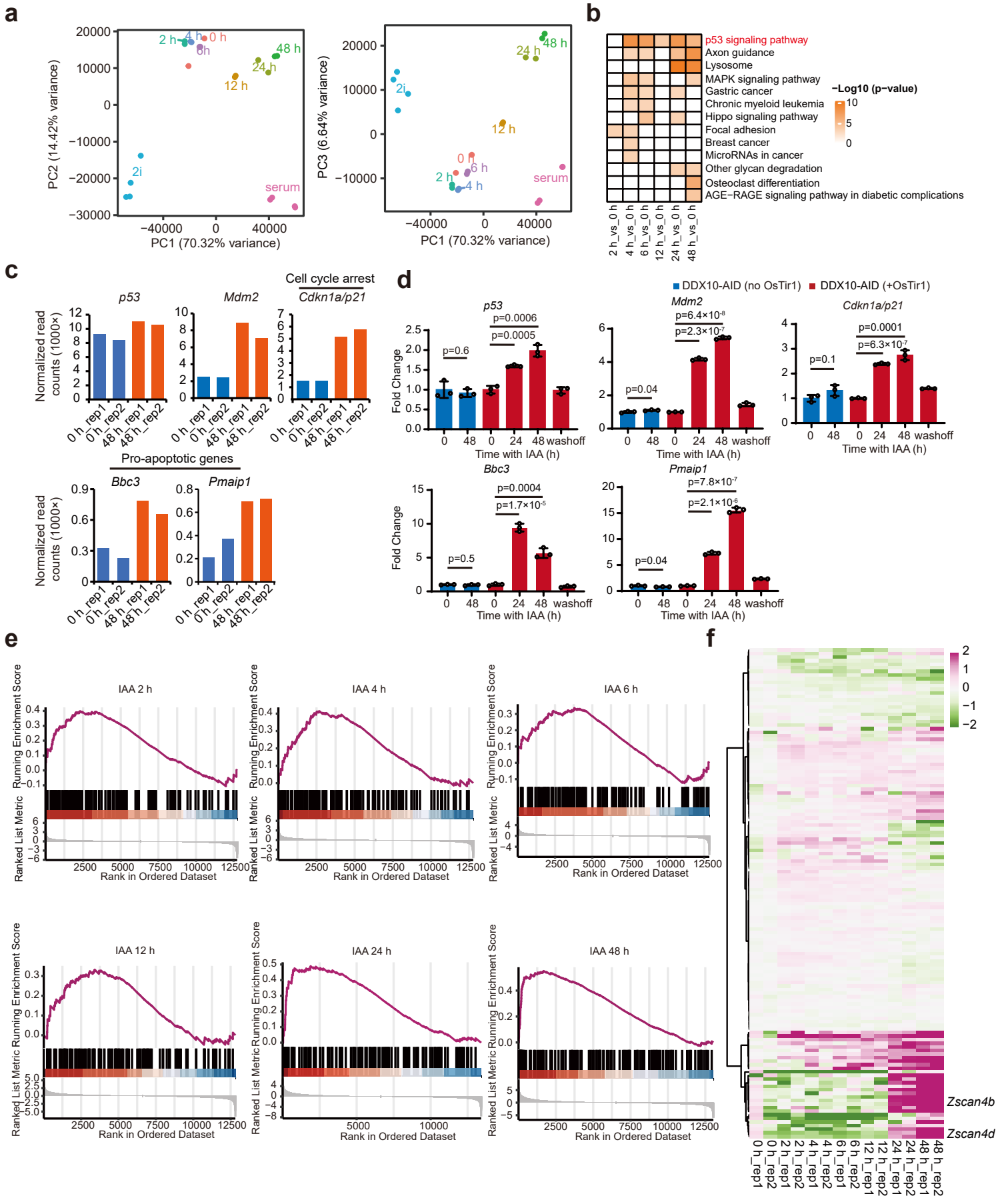
Uncropped gel and blots.

Supplementary Figure 1



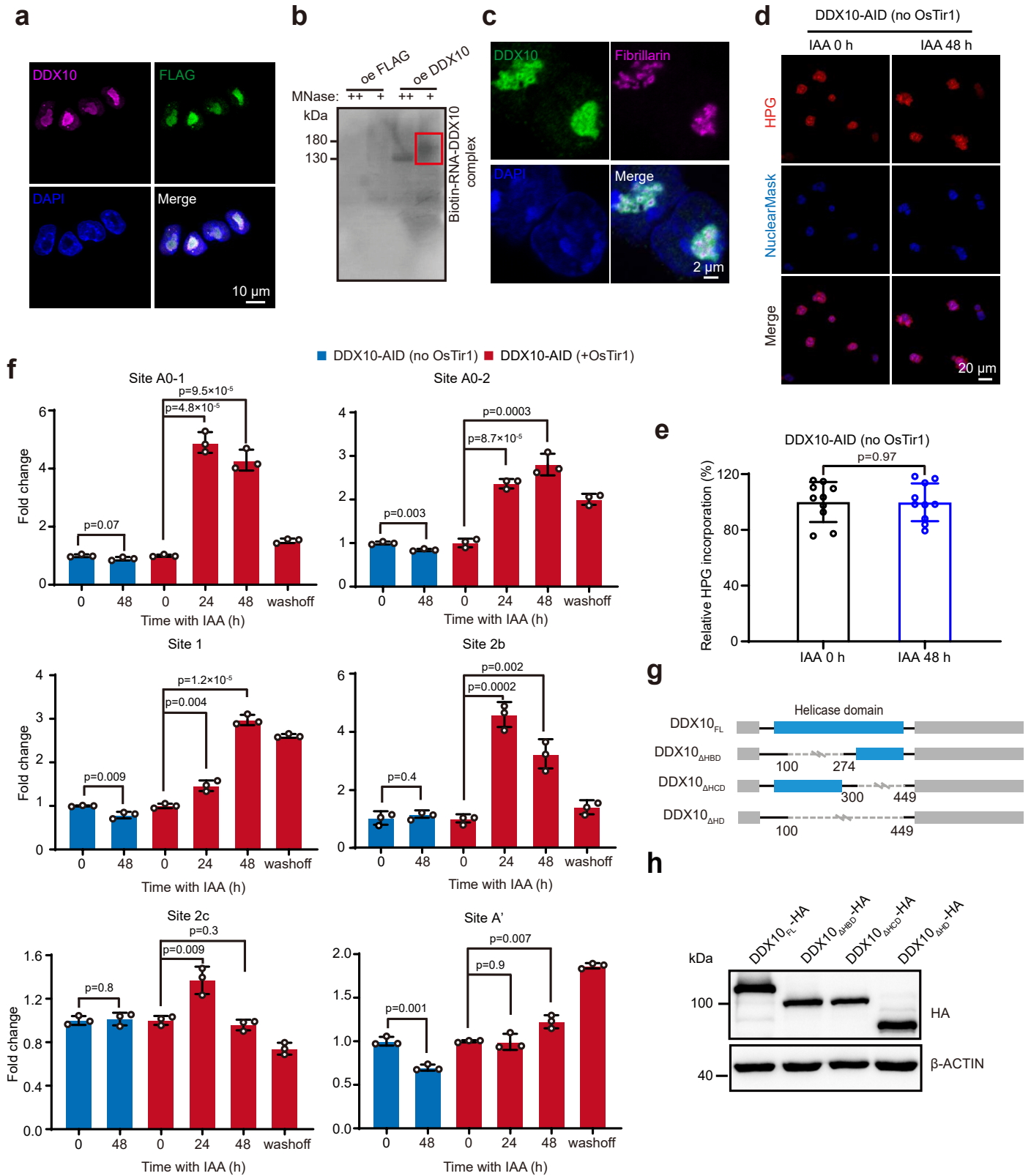
Supplementary Figure 1. DDX10 depletion and its effects on mESC growth, cell cycle, and apoptosis. **a** Left panel: Schematic representation of the homologous recombination strategy to introduce an AID-eGFP tag in the endogenous *Ddx10* gene. Middle panel: Validation of homozygous integration using PCR. Right panel: Sanger sequencing confirming in-frame tagging of AID-eGFP tag. **b** Fluorescence microscopy images showing GFP in DDX10-AID (+OsTir1) mESCs treated with IAA (0 h, 24 h, and 48 h) and treated with IAA for 48 h followed by 48 h of washing. Experiments were repeated three times independently with similar results. Scale bar, 100 μ m. **c** Flow cytometry analysis of GFP fluorescence in DDX10-AID (+OsTir1) mESCs with IAA treatment at different time points. $n = 3$ independent experiments. **d** Clonal morphology of wild-type and DDX10-AID (+OsTir1) mESCs. Scale bar, 200 μ m. **e** Cell cycle analysis of wild-type and DDX10-AID (+OsTir1) mESCs. **f** FACS analysis of apoptosis in wild-type and DDX10-AID (+OsTir1) mESCs. $n = 3$ independent experiments. **g** Colony areas of DDX10-AID (+OsTir1) mESCs with IAA treatment at different time points (0 h, 24 h, and 48 h), and with IAA treatment for 48 h followed by 48 h of washing. The number of cells for statistical analysis (n) is indicated in the figure. **h** Western blot analysis of OCT4, NANOG, SOX2, and DDX10 in DDX10-AID (+OsTir1) cells without or with IAA treatment at different time points. β -ACTIN was used as a loading control. Experiments were repeated three times independently with similar results. **i** Cell number count of DDX10-AID (+OsTir1) mESCs treated with IAA at different time points (day 0, 1, 2, and 4) and treated with IAA for 48 h, followed by 48 h of washing. **j** Cell viability was assessed using CCK8 assay in DDX10-AID (+OsTir1) and control mESCs with IAA treatment at different time points (day 0, 1, 2, and 4) and with IAA treatment for 48 h followed by 48 h of washing. DDX10-AID: DDX10-AID (+OsTir1) mESCs; Ctrl: DDX10-AID (no OsTir1) mESCs. **k** Cell cycle distribution analysis of DDX10-AID (+OsTir1) cells treated with IAA at different time points (0 h, 24 h, and 48 h) and with IAA treatment for 48 h followed by 48 h of washing. $n = 3$ independent experiments. **l** Quantification of FACS data shown in (**k**). **m** Flow cytometric analysis of apoptosis in DDX10-AID (+OsTir1) cells treated similarly as in (**k**). $n = 3$ independent experiments. **n** Quantification of FACS data shown in (**m**). For panel **g**, **i**, **j**, **l** and **n**, data are presented as mean values \pm SD with the indicated significance from two-sided t test. Exact p values are reported in the figure. $n = 3$ independent experiments. Source data are provided as a Source Data file.

Supplementary Figure 2



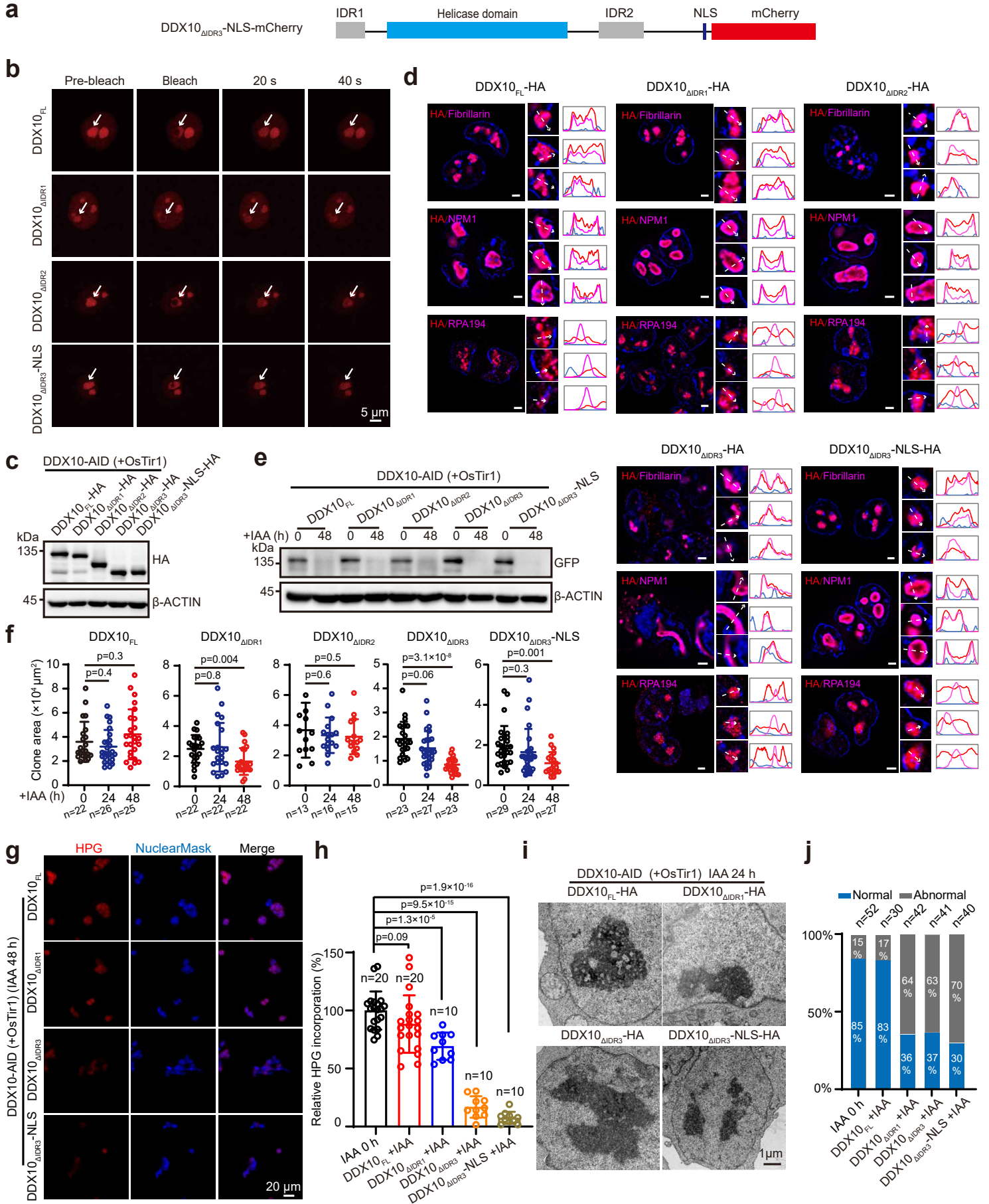
Supplementary Figure 2. DDX10 depletion activates the p53 signal pathway and induces the expression of 2-cell specific genes. **a** PCA analysis of RNA-seq data from GSE226316 and our RNA-seq data. **b** KEGG pathway enrichment analysis highlighting upregulated genes following DDX10 degradation. **c** Bar plot depicting normalized read counts for *p53*, *Mdm2*, *Cdkn1a/p21*, *Bbc3*, and *Pmaip1* expression in DDX10-AID mESCs treated with or without IAA based on RNA-seq data. **d** RT-qPCR analysis of the expression levels of *p53* and its related genes *Cdkn1a/p21*, *Mdm2*, *Bbc3*, and *Pmaip1* in DDX10-AID mESCs treated with IAA at different time points. Transcription levels were normalized against *Gapdh*. Data are shown as mean values \pm SD with the indicated significance from two-sided *t* test. Exact p values are reported in the figure. *n* = 3 independent experiments. **e** Gene set enrichment analysis (GSEA) of 2-cell specific genes in RNA-seq data after DDX10 degradation. **f** Heatmap presenting the expression of 2-cell specific genes with IAA treatment at different time points. Source data are provided as a Source Data file.

Supplementary Figure 3



Supplementary Figure 3. Nucleolar localization and role of DDX10 in pre-rRNA processing. **a** Immunofluorescence staining of DDX10 (magenta) and FLAG (green) in FLAG-tagged DDX10 mESCs. Nuclei were stained with DAPI. Experiments were repeated three times independently with similar results. Scale bar, 10 μ m. **b** Biotin-labeled RNA imaging of DDX10 CLIP. Biotin-labeled protein-RNA complexes were separated on a NuPAGE Bis-Tris protein gel and transferred to a nitrocellulose membrane. ++ represents 10^3 times dilution of MNase; + represents 5×10^5 times dilution of MNase. Experiments were repeated three times independently with similar results. **c** Immunofluorescence staining of DDX10 (green) and Fibrillarin (magenta) in mESCs. Nuclei were stained with DAPI. Experiments were repeated three times independently with similar results. Scale bar, 2 μ m. **d** HPG incorporation analyzing nascent protein synthesis in DDX10-AID (no OsTir1) mESCs at 0 h and 48 h after IAA treatment. Experiments were repeated two times independently with similar results. Scale bar, 20 μ m. **e** Quantification of relative HPG incorporation shown in (d). Data are shown as mean values \pm SD with the indicated significance from two-sided *t* test. Exact p values are reported in the figure. n = 10 fields. **f** RT-qPCR analysis of pre-rRNA processing intermediates upon IAA treatment in DDX10-AID and control cells. Transcription levels were normalized against *Gapdh*. Data are shown as mean values \pm SD with the indicated significance from two-sided *t* test. Exact p values are reported in the figure. n = 3 independent experiments. **g** Schematic representation of different truncations of mouse DDX10 lacking helicase domain region. **h** Western blot showing the protein levels of DDX10_{FL} and its various truncations. Experiments were repeated three times independently with similar results. Source data are provided as a Source Data file.

Supplementary Figure 4



Supplementary Figure 4. DDX10 undergoes phase separation. **a** Schematic diagram of DDX10 $_{\Delta IDR3}$ -NLS-mCherry. **b** Representative images of fluorescence recovery in NIH3T3 cells. White arrows indicate the bleached areas. Experiments were repeated three times independently with similar results. Scale bars, 5 μ m. **c** Western blot showing the protein levels of DDX10 $_{FL}$ and different truncations. Experiments were repeated three times independently with similar results. **d** Representative SIM images of HA (red), GC marker NPM1 (magenta), DFC marker Fibrillarin (magenta), and FC marker RPA194 (magenta) in mESCs. Experiments were repeated three times independently with similar results. Scale bar, 2 μ m. **e** Western blot showing the protein levels of GFP (DDX10-AID-eGFP) in DDX10-AID cells without or with IAA treatment for 48 h. Experiments were repeated two times independently with similar results. **f** Colony areas of mESCs overexpressing DDX10 $_{FL}$, DDX10 $_{\Delta IDR1}$, DDX10 $_{\Delta IDR3}$, or DDX10 $_{\Delta IDR3}$ -NLS at different time points (0 h, 24 h, and 48 h) after IAA treatment. The number of cells for statistical analysis (n) is indicated in the figure. Data are shown as mean values \pm SD with the indicated significance from two-sided *t* test. Exact p values are reported in the figure. **g** HPG incorporation analyzing nascent protein synthesis in DDX10-AID (+OsTir1) mESCs overexpressing DDX10 $_{FL}$, DDX10 $_{\Delta IDR1}$, DDX10 $_{\Delta IDR3}$, or DDX10 $_{\Delta IDR3}$ -NLS, respectively, after 48 h of IAA treatment. Experiments were repeated three times independently with similar results. Scale bar, 20 μ m. **h** Quantification of relative HPG incorporation shown in (g). The number of fields for statistical analysis (n) is indicated in the figure. Data are shown as mean values \pm SD with the indicated significance from two-sided *t* test. Exact p values are reported in the figure. **i** TEM images showing the nucleolar structure of DDX10-AID (+OsTir1) mESCs overexpressing DDX10 $_{FL}$, DDX10 $_{\Delta IDR1}$, DDX10 $_{\Delta IDR3}$, or DDX10 $_{\Delta IDR3}$ -NLS, respectively, after 24 h of IAA treatment. Experiments were repeated two times independently with similar results. Scale bar, 1 μ m. **j** Bar graphs showing the percentage of cells with normal or abnormal GC/DFC/FC structure. Source data are provided as a Source Data file.

Uncropped gels and blots

Fig. 1e

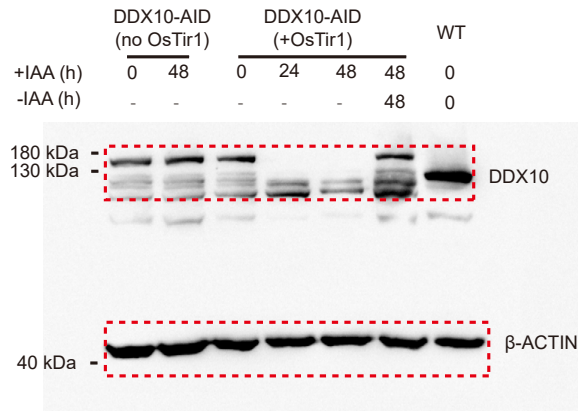


Fig. 3g

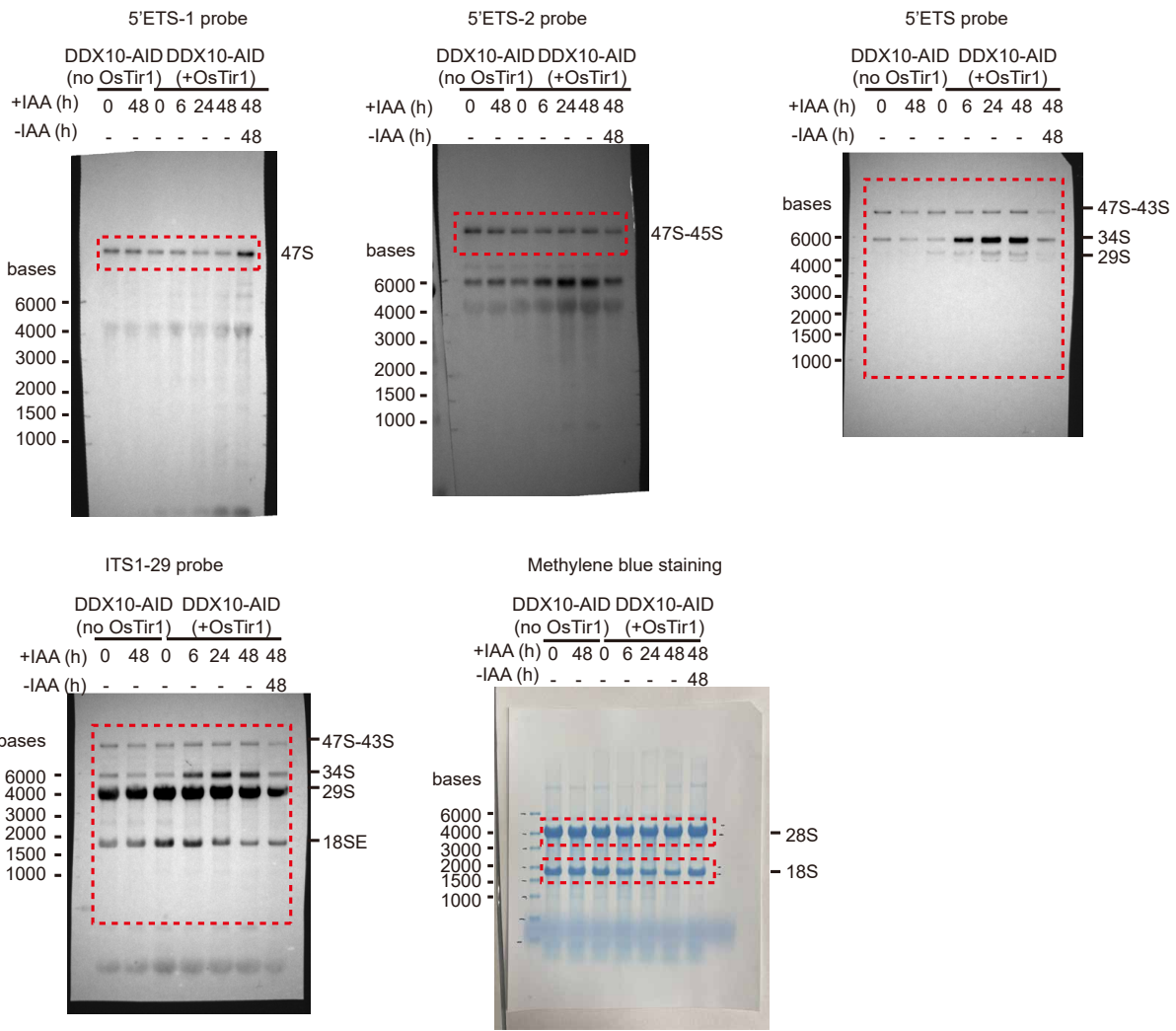


Fig. 3h

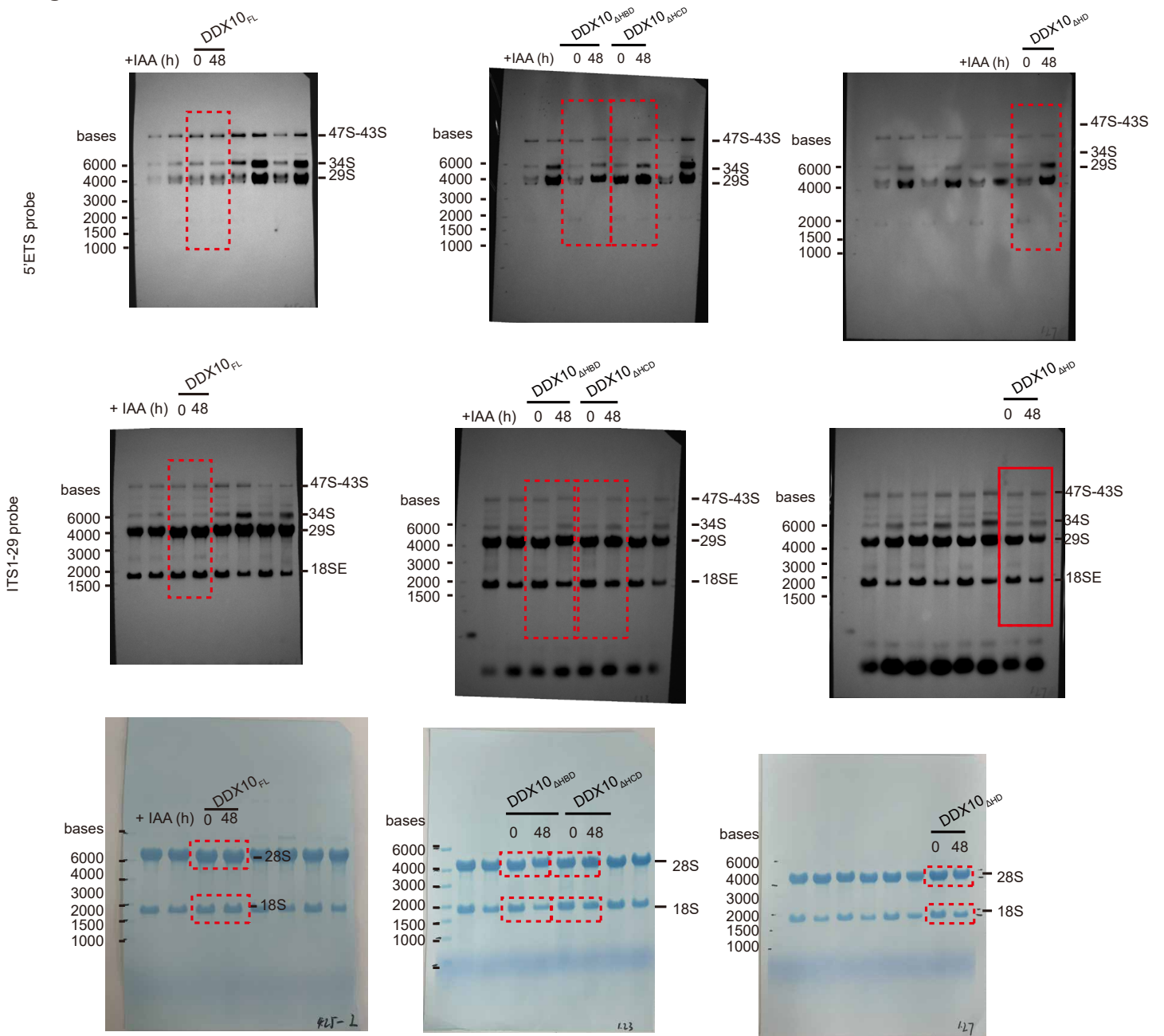


Fig. 4a

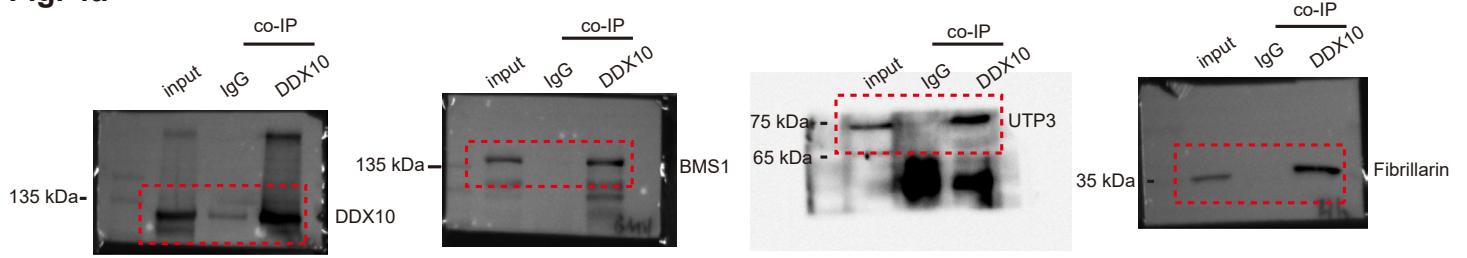


Fig. 4c

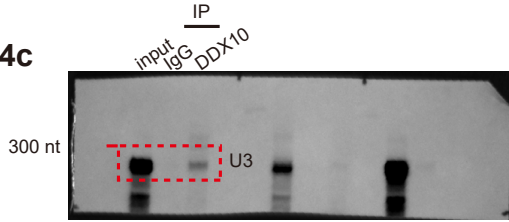


Fig. 4e

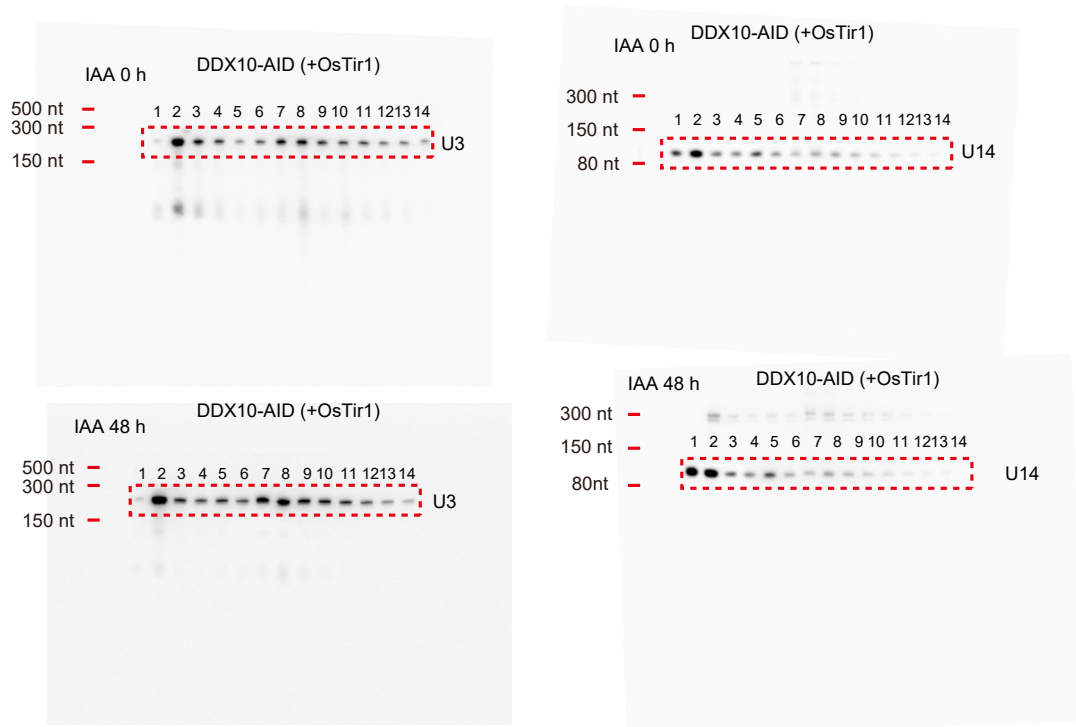


Fig. 4f

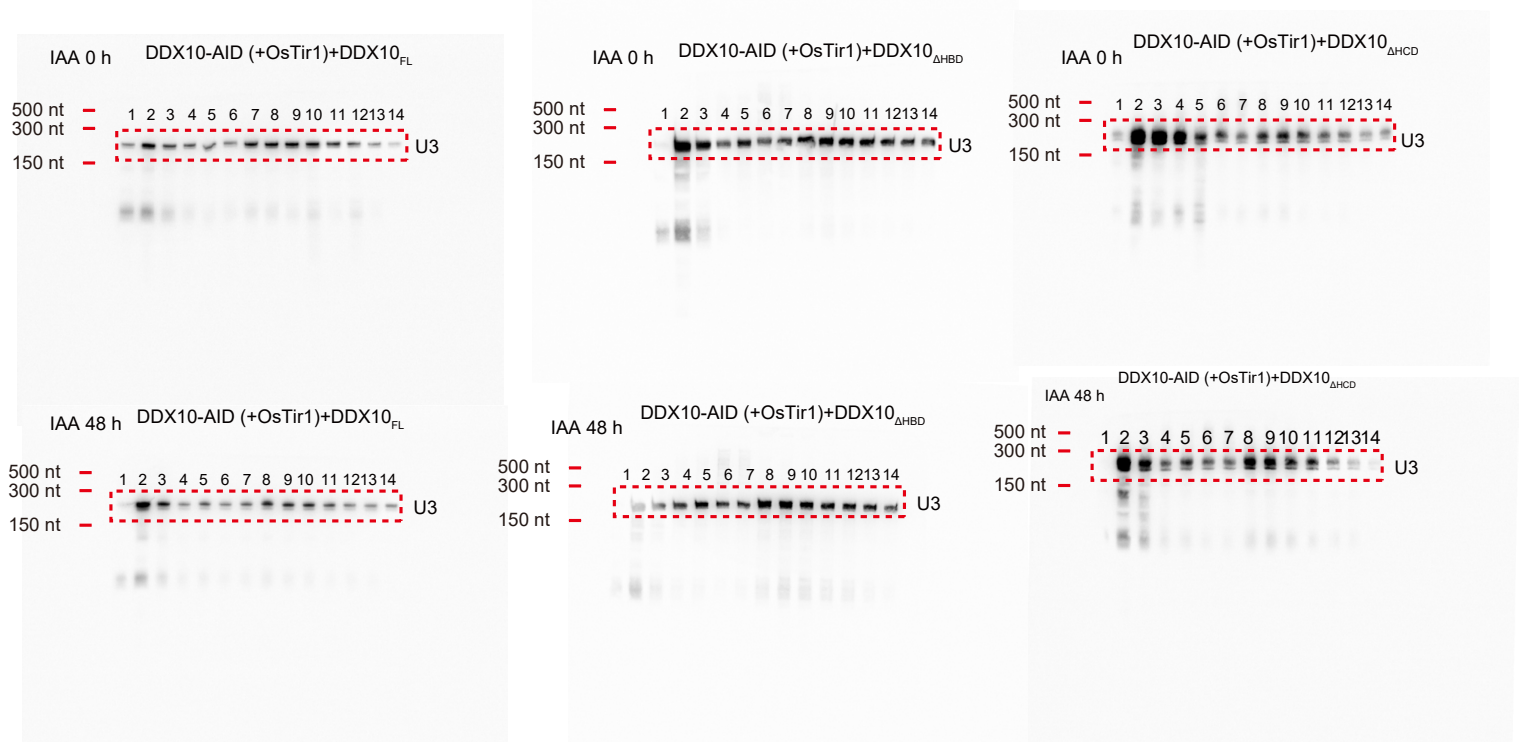


Fig. 5i

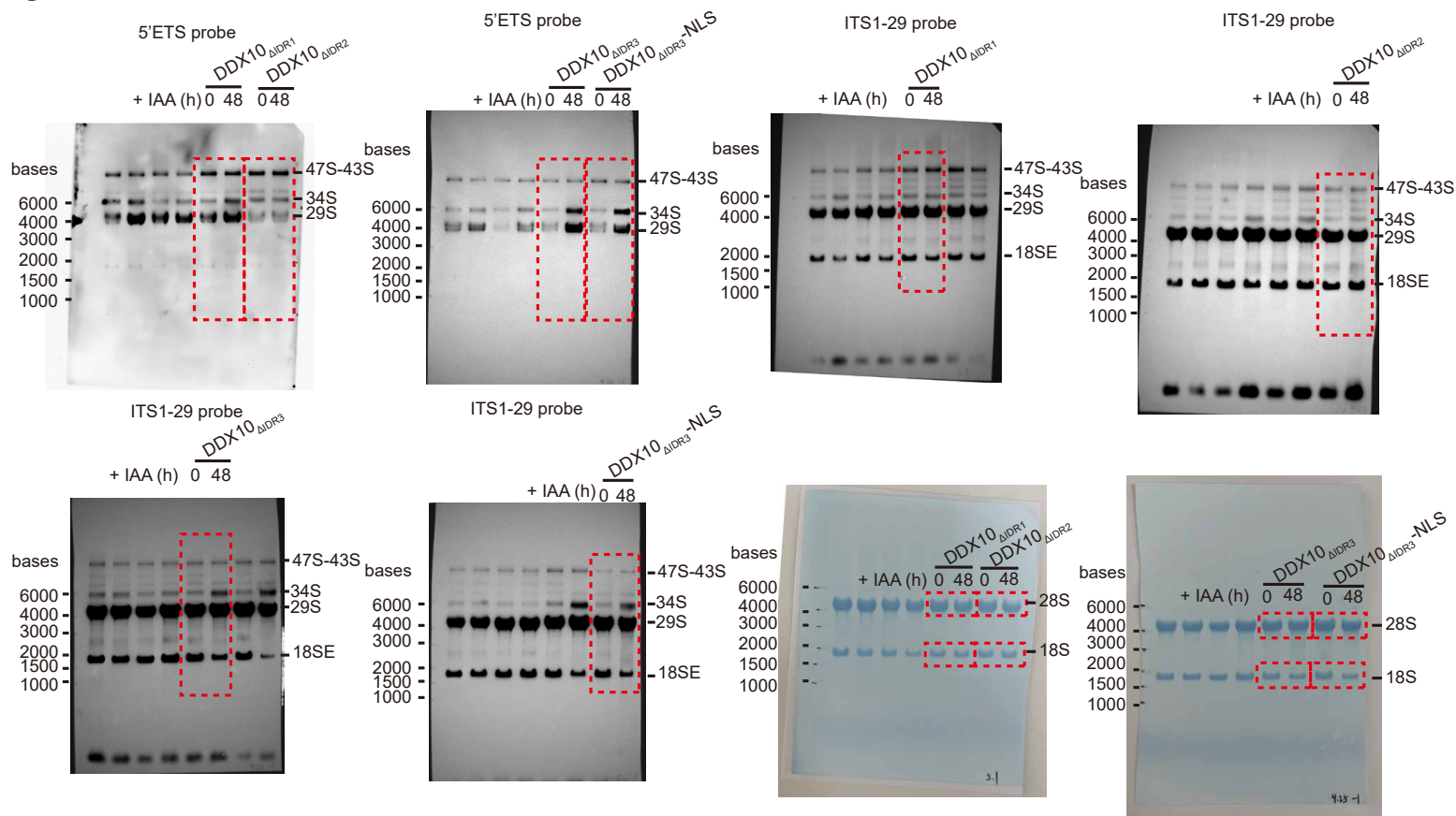


Fig. 5j

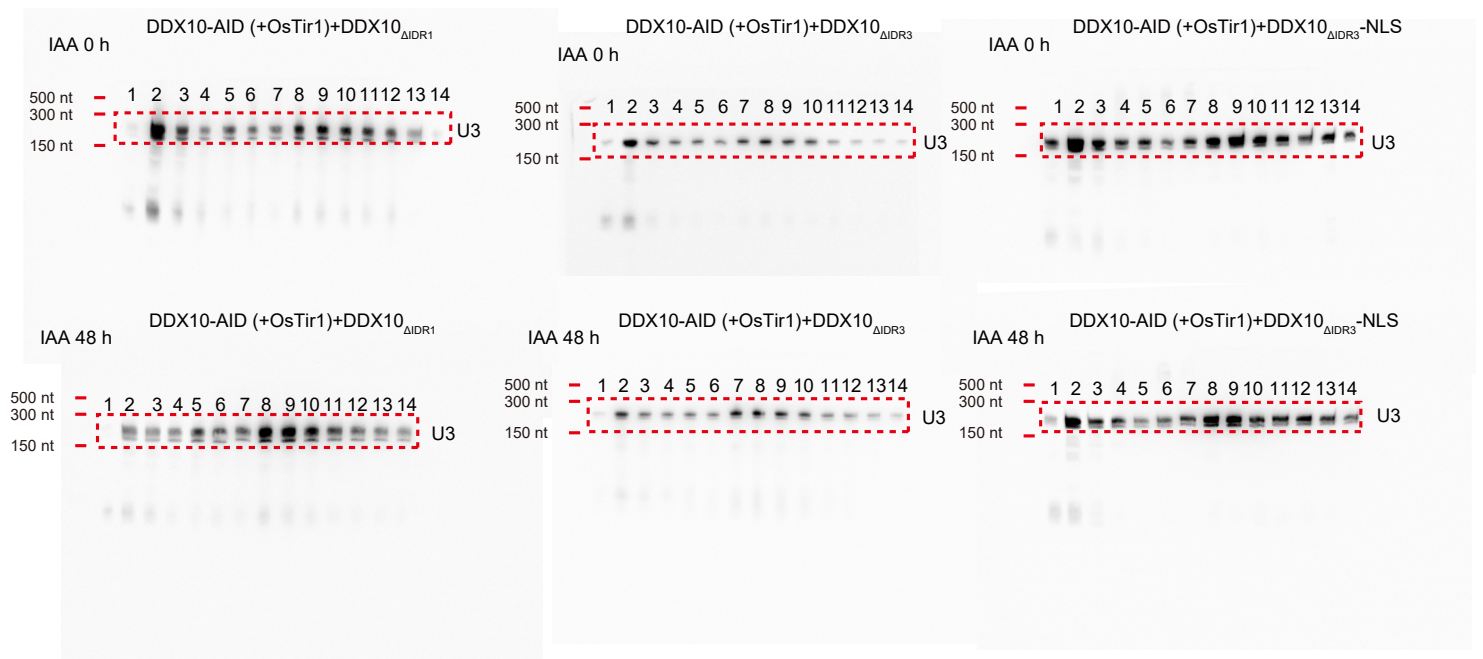


Fig. 6b

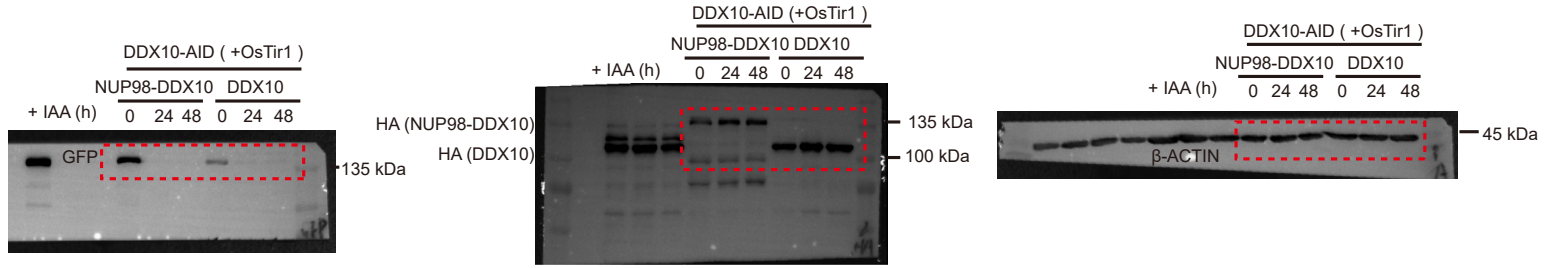
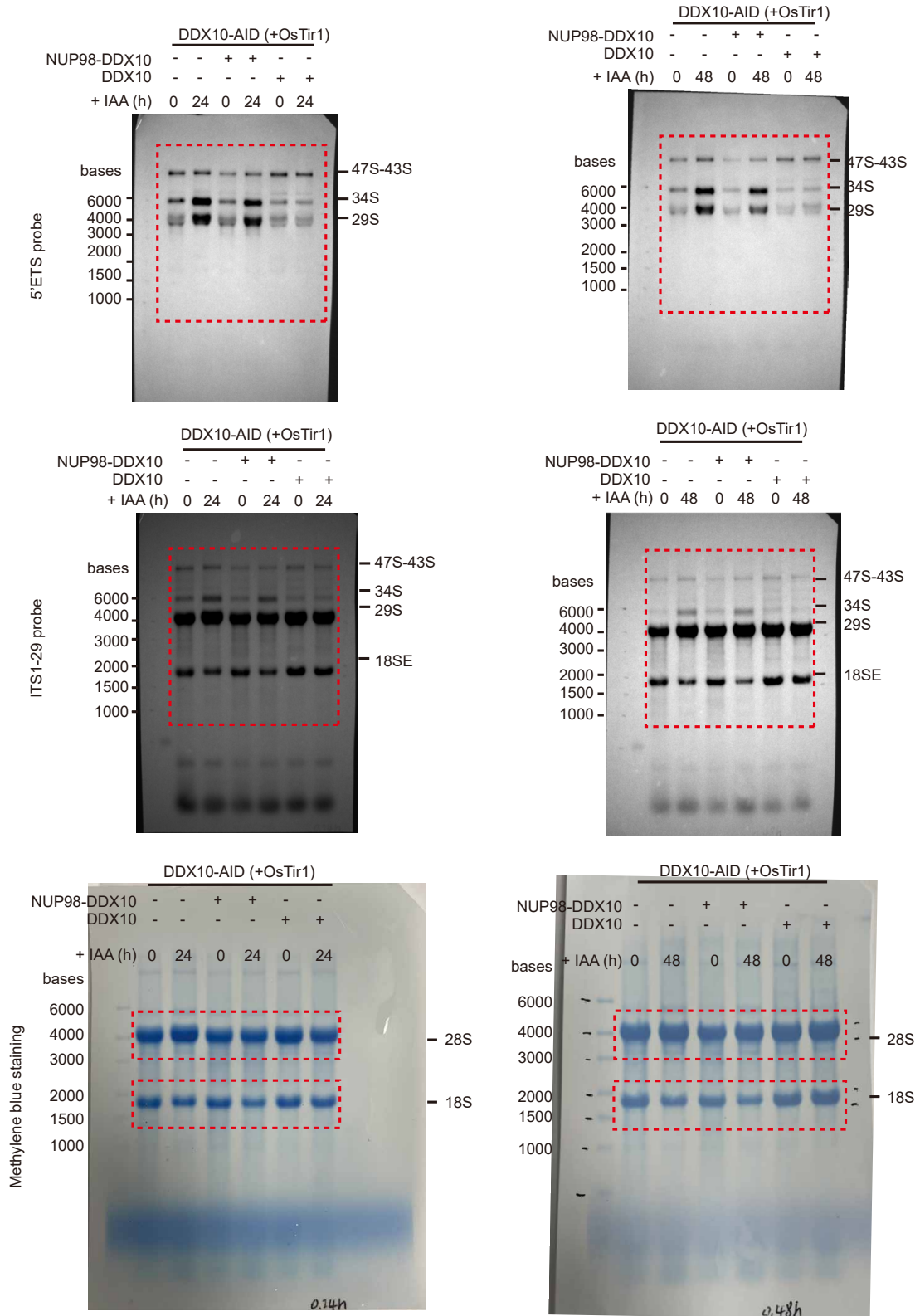
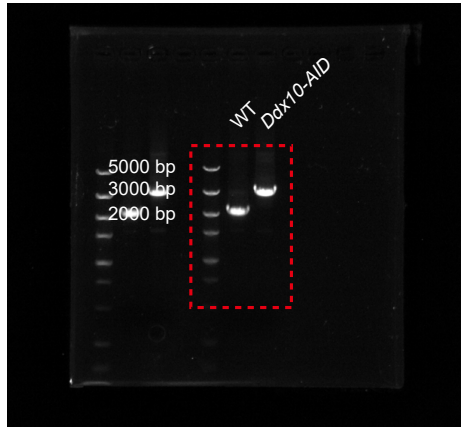


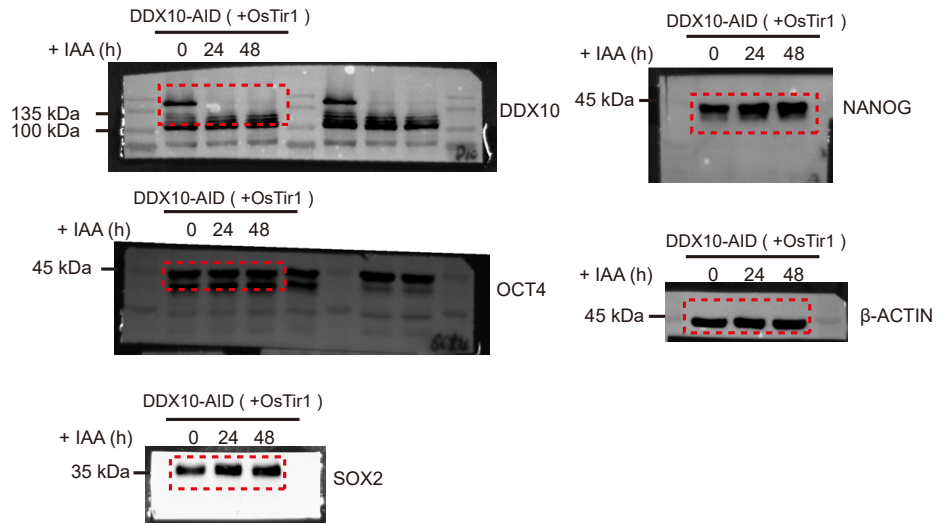
Fig. 6f



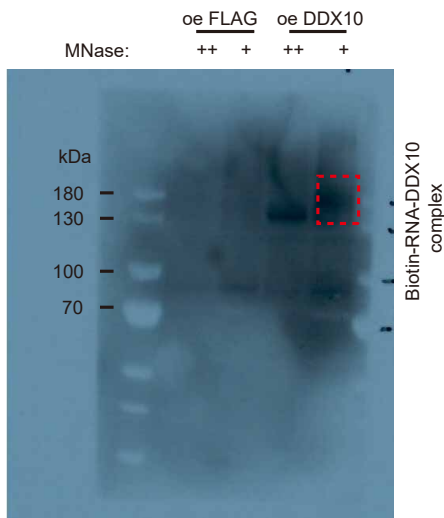
Supplementary Fig.1a



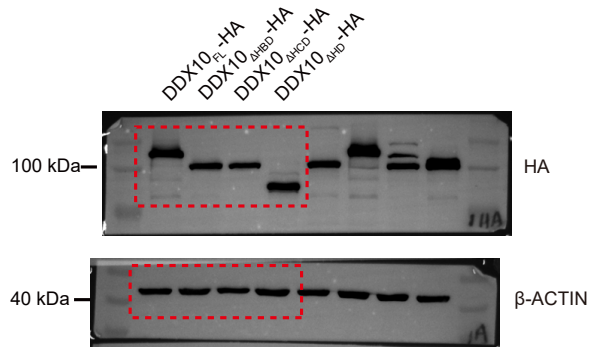
Supplementary Fig. 1h



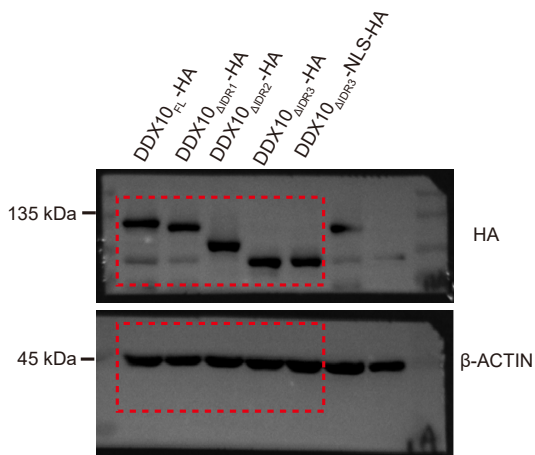
Supplementary Fig. 3b



Supplementary Fig. 3h



Supplementary Fig. 4c



Supplementary Fig. 4e

